Physics Letters B 694 (2011) 316–321

Contents lists available at ScienceDirect

Physics Letters B

www.elsevier.com/locate/physletb

Quadrupole moment of the 6^- isomeric state in ^{66}Cu: Interplay between different nuclear deformation driving forces

R.L. Lozeva [a,b,*], D.L. Balabanski [c], G. Georgiev [a], J.-M. Daugas [d], S. Péru [d], G. Audi [a], S. Cabaret [a], T. Faul [d], M. Ferraton [e], E. Fiori [a], C. Gaulard [a], F. Ibrahim [e], P. Morel [d], L. Risegari [a], D. Verney [e], D.T. Yordanov [f]

[a] CSNSM, Université Paris-Sud 11, CNRS, IN2P3, F-91405 Orsay-Campus, France
[b] IPHC, CNRS, IN2P3, F-67037 Strasbourg Cedex 2, France
[c] INRNE, Bulgarian Academy of Sciences, BG-1784 Sofia, Bulgaria
[d] CEA, DAM, DIF, F-91297 Arpajon Cedex, France
[e] IPN, CNRS, IN2P3, F-91406 Orsay-Campus, France
[f] Max-Planck-Institut für Kernphysik, D-69117 Heidelberg, Germany

ARTICLE INFO

Article history:
Received 10 May 2010
Received in revised form 10 September 2010
Accepted 8 October 2010
Available online 14 October 2010
Editor: V. Metag

Keywords:
Electromagnetic moments
Angular distribution and correlation measurements
Nucleon transfer reactions
Nuclear MF model

ABSTRACT

We have measured the spectroscopic quadrupole moment of the 6^- isomeric state in ^{66}Cu to be $|Q_s| = 18.6(12)$ efm^2. This state results from a weak coupling of the $\pi p_{3/2}$ and the $\nu g_{9/2}$ orbitals, which lead to sizable deformation at oblate and prolate shapes, correspondingly, in the ^{68}Ni region. The interplay between these two different deformation-driving orbitals is observed at $N = 37$ for the 6^- state resulting in a most probable oblate shape.

1. Introduction

Nickel is the only element in nature which has three known isotopes that are doubly magic nuclei (^{48}Ni, ^{56}Ni and ^{78}Ni). The common understanding is that a gradual change of the shape of these nuclei appears between each two magic shells. Recently, the nuclei in the vicinity of ^{68}Ni were studied extensively since they yield important information about the shell structure away of stability and the onset of deformation, based on the experimental evidences from the 2_1^+ excitation energies and their $B(E2)$ transition rates [1,2]. For this region it has been predicted that where nuclear deformation sets in, the magic numbers disappear, leading to very localized effects as the sub-shell closure at $N = 40$ [3,4]. There are few experimental evidences for deformed shapes as in ^{66}Fe [5] and shape changes from prolate in ^{55,57}Cr [6] to oblate at $N = 35$ for ^{59}Cr [7,8]. According to theoretical predictions the shape changes to prolate in ^{60,62}Cr [9], is strongly deformed in ^{64}Cr [9], reduces deformation in the heavier Fe isotopes [10] and favours the prolate form for ^{66}Fe [9,11]. These facts suggest that when two (or more) identical particles/holes are coupled to the ^{68}Ni core, its stabilizing effect disappears. This leads to: (i) onset of deformation, and hints of shape coexistence below Ni [12–14]; (ii) low-lying predominantly single-particle states in the Fe and the neutron-rich Cu isotopes e.g. $^{69-71}$Cu from particle–hole excitations across the $Z = 28$ gap [15]; (iii) collectivity in the nuclei above Ni as e.g. ^{73}Cu [16]. The intriguing character of the deformation behaviour is a consequence of the interaction between the $g_{9/2}$ neutron particles and $f_{7/2}$ proton holes, that leads to a (dramatic) lowering [9,13,17] of the $\nu g_{9/2}$ orbital (or an effective rise in the $\pi f_{7/2}$ due to the tensor force in the *pn* interaction [18]). Because of the $\nu g_{9/2}$ lowering with increasing N, beyond 36, the down-sloping $\nu[440]1/2^+$ and $\nu[431]3/2^+$ orbitals are more likely to be occupied than the spherical orbitals. This generates a region around $N = 40$ with an increased deformation, where the configuration functions of the nuclear states involve proton holes in $f_{7/2}$ and neutrons in $g_{9/2}$ [5]. Magnetic moment measurements in ^{69}Cu and ^{63,65,67}Ni isotopes [19,20] show considerable contributions of excitations across the $\pi f_{7/2}$ shell and hint for deviation from sphericity only one hole away from ^{68}Ni. A sizable quadrupole de-

* Corresponding author at: IPHC, CNRS, IN2P3, F-67037 Strasbourg Cedex 2, France.
E-mail address: Radomira.Lozeva@iphc.cnrs.fr (R.L. Lozeva).

0370-2693
doi:10.1016/j.physletb.2010.10.016

formation ($\beta_2 \geqslant 0.25$) has been reported in β-decay studies of ^{67}Co [14] based on the observation of a prolate $(1p$–$2h)$ proton intruder $(\pi[321]1/2^-)$ first excited state. It is obtained by promoting one proton particle from the $\pi f_{7/2}$ into the $\pi p_{3/2}$ orbital [14], a configuration that is favoured also by the neutrons because of the sharply down-sloping $\nu[440]1/2^+$ and $\nu[431]3/2^+$ orbitals. In this region very few direct measurements on the nuclear deformation were performed. Such are the studies on the quadrupole moments in ^{63,65}Cu [29,30] and ^{61m}Fe [22]. In the former ones, the main contribution comes from a single proton in the $\pi p_{3/2}$ orbital, coupled to the semi-magic Ni core, leading to a sizable oblate shape. The only experimental result from an odd neutron in the $\nu g_{9/2}$ orbital is for the ^{61m}Fe$(9/2^+)$ isomer, revealing a large variation from sphericity [22].

This Letter reports on the first direct determination of the nuclear deformation involving both, the $\pi p_{3/2}$ and the $\nu g_{9/2}$ orbitals in this region by measuring the spectroscopic quadrupole moment of the 6^- isomeric state ($E_x = 1154$ keV, $T_{1/2} = 595(20)$ ns) [23] in ^{66}Cu. In addition, it provides an important test for the experimental methodology to study the quadrupole moments of nuclei, aligned in a reaction of nucleon transfer.

2. Experimental technique

The ^{66}Cu nuclei were produced in a (d, p) reaction by a pulsed 6 MeV ^{2}H beam (pulse width of $\leqslant 2$ ns, repetition rate of 5 µs and mean intensity of about 0.4 nA ($\sim 2 \times 10^9$ p/s)) on a Cu_2O target at the Tandem-ALTO facility of Orsay. The spin alignment of the isomers of interest was obtained in the transfer reaction. At the same time the target was used as a host providing an electric field gradient (EFG) for the quadrupole interaction. It was prepared from 99.0(1)% purity polycrystalline cuprous oxide powder under a pressure of ∼100 MPa, which is well below the phase-change threshold of 10 GPa [24] to assure no affect on the crystalline structure. The resulted target thickness is of ∼700 µm with a density of ∼5.4 g/cm^3. The detection set-up consisted of 8 HPGe single crystal detectors, placed at a distance of ∼10 cm from the target, resulting in a total detection efficiency of about 5% at 1.3 MeV. Time–γ correlations were recorded in the 2.5 MeV energy and 5 µs time range. The later were triggered by γs and stopped by the beam pulsing. The time resolution of the Ge detectors was of the order of 15 ns. Six of the detectors were positioned in a horizontal plane at ±30°, ±90°, ±150° with respect to the beam direction, while the other two were placed top/bottom at ±90° with respect to the horizontal plane.

The perturbed angular distribution with quadrupole interactions for a polycrystalline host can be expressed by:

$$W(\theta, t) = \sum_k A_k B_k G_{kk}(t) P_k\big(\cos(\theta)\big), \tag{1}$$

where A_k are the angular distribution coefficients dependent on the multipolarity of the observed radiation, B_k are the orientation coefficients, that depend on amount of spin-alignment of the isomeric ensemble, G_{kk} are perturbation factors dependent on the EFG, the crystalline structure of the host and the spin of the investigated state, and $P_k(\cos(\theta))$ are the Legendre polynomials [25]. Note that this expression is valid for any detector, placed at an angle θ with respect to the alignment axis, and independent of the angle ϕ or of its horizontal or vertical placement. The G_{kk} factors are connected to the s_{kn} coefficients, associated to the transitions between magnetic sub-states induced by the quadrupole interaction by:

$$G_{kk} = \sum_{n>0} s_{kn} \cos(n w_0 t), \tag{2}$$

where for aligned nuclei only even k values are considered [26]. Thus, $W(\theta, t)$ simplifies to the main contributions of $A_{2,4}$, $B_{2,4}$ and $G_{22,44}$.

The Time Dependent Perturbed Angular Distribution (TDPAD) technique was used to observe the change in the γ-ray angular distribution $W(\theta, t)$ [27,26]. Its maximum could be observed for detectors at $\theta = 0°$ and minimum for detectors at $\theta = 90°$ with respect to the symmetry axis of the spin-alignment which in this case coincides with the beam axis. An $R(t)$ function was constructed using the γ-ray intensities of detectors at different angles:

$$R(t) = \frac{W(30°, t) - \epsilon W(90°, t)}{W(30°, t) + \epsilon W(90°, t)}, \tag{3}$$

where ϵ is an efficiency normalization factor. We note that in this case, the detectors were positioned at 30° instead of 0° which coincides with the beam axis. This lead to a reduction of the $R(t)$ amplitude of about 28%.

The experimental $R(t)$ function was further used for the determination of the quadrupole coupling constant, ν_Q (called often only a quadrupole frequency), directly related to the spectroscopic quadrupole moment, Q_s, of the isomeric state:

$$\nu_Q = eQ_sV_{zz}/h, \tag{4}$$

where V_{zz} is the principal component of the EFG at the nuclear site. The observed quadrupole frequency, w_0, is related to the oscillation (quadrupole) frequency, ν_Q^0, as $w_0 = 2\pi\nu_Q^0$ which itself is related to the quadrupole coupling constant as following:

$$\nu_Q^0 = \frac{3i\nu_Q}{4I(2I-1)}, \tag{5}$$

where $i = 1$ for integer spin, I, and $i = 2$ for half-integer I. Note that V_{zz} does not depend on the isotope but only on its atomic number. Thus, knowing V_{zz} for an element in a particular material, one can perform measurements of the quadrupole interaction for all of its isotopes.

The quadrupole oscillation frequencies, ν_Q^0, of ^{63}Cu and ^{65}Cu in Cu_2O were determined in an NQR measurement as 26.001(14) MHz and 24.069(14) MHz (at 295 K) [28], respectively. Q_s of ^{63}Cu$(3/2^-)$ ground state (g.s.) is known from an optical spectroscopy measurement as $Q_s = -21.1(4)$ efm^2 [29] and from a muon X-ray hyperfine structure measurement as $|Q_s| = 22.0(15)$ efm^2 [30]. Thus, we adopt a value of $Q_s = -21.2(4)$ efm^2. For the ^{65}Cu$(3/2^-)_{g.s.}$ the reported value amounts to $Q_s = -19.5(4)$ efm^2 [29]. Knowing ν_Q^0 and Q_s, we determined V_{zz} of Cu in Cu_2O from ^{63}Cu as $V_{zz} = 101.5(19) \times 10^{20}$ V/m^2 and from ^{65}Cu as $V_{zz} = 102.1(21) \times 10^{20}$ V/m^2. Therefore, for the strength of the EFG we adopt a value of $V_{zz} = 101.8(14) \times 10^{20}$ V/m^2. It is in agreement with the value deduced in [31] using the same methodology, however not taken as a reference, as in that work $Q_s(^{63}\text{Cu}, 3/2^-)$ without a Sternheimer correction has been used [29].

The form of the $R(t)$ function depends whether the nuclei are implanted in a single or a polycrystal. In the unit cell of Cu_2O there are four different Cu atoms with the EFG along the four indistinguishable [111] directions forming a polycrystalline structure [32]. Each of these axes is at about 54.7° with respect to the principle axes. As there is no selective implantation into one of these, the experimental perturbation function in the polycrystal is a superposition (ensemble) of the four different single crystals. This results in an undefined (random) orientation of V_{zz}, with well-defined TDPAD pattern. Therefore, a normal integration is possible for a Q_s measurement. The sign of Q_s cannot be determined experimentally, if a spin-aligned ensemble is used. In order to measure the sign, one needs a spin-polarized ensemble and well-defined direction (and sign) of the EFG [33,34].

3. Experimental results

The 6^- isomeric state of interest in ^{66}Cu with $T_{1/2} = 595(20)$ ns was observed in a ^{65}Cu(d, p) reaction [23], to decay by five γ-ray transitions, as shown in Fig. 1(a). The spin/parity (I^π) of the state was assigned by measuring its magnetic moment ($\mu = +1.038(3)$ n.m.) [23]. It was well explained by additive coupling of the $\mu_\pi(3/2^-)$ and $\mu_\nu(9/2^-)$, taken from neighbouring odd–even and even–odd nuclei, suggesting $(\pi p_{3/2} \otimes \nu g_{9/2})6^-$ configuration.

A typical delayed and background-subtracted γ-ray spectrum from the current data set is displayed in Fig. 1(b) where we clearly observe four of the known isomeric transitions: 563, 316, 186 and 89 keV. The multipolarities of these γ-rays were suggested to be predominantly $6^-(M2)4^+(M1)3^+(M1)2^+(M1)1^+$ [23]. The time spectrum, shown in Fig. 1(c), represents the data from all four isomeric transitions detected in all detectors, fitted with a single decay component after a constant background is subtracted. The experimentally obtained isomeric half-life $T_{1/2} = 601(30)$ ns includes statistical uncertainties of the fits for each transition separately, and is in a very good agreement with [23].

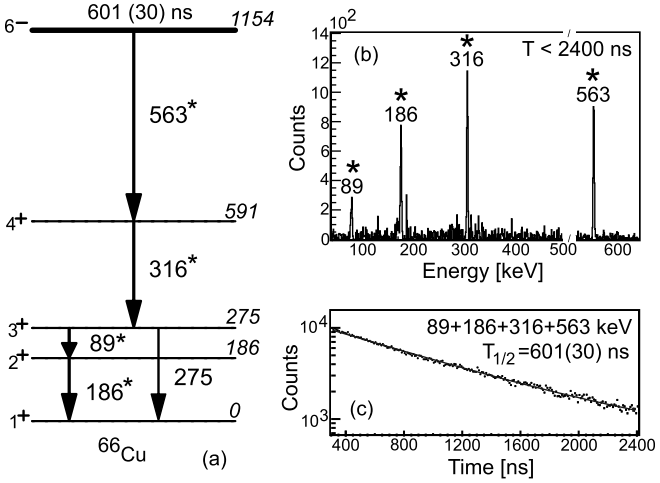

Fig. 1. The decay scheme of the 6^- isomer in ^{66}Cu (a) and a typical delayed and background-subtracted γ-ray spectrum (b), where all observed isomeric transitions are indicated with asterisks. Sum-up background-subtracted time spectrum (in a logarithmic scale) for all observed transitions with its fit (c).

GEANT simulation [35] was performed using a realistic set-up in the actual experimental geometry. The angular distribution $W(\theta, t)$ was simulated following the formalism in [26,25]. The $R(t)$ function was constructed from the combination of detectors at 30° and at 90° with respect to the beam axis using Eq. (3). Therefore, the sum-up spectrum of all detectors represents the combination of all placed at ±30° and at ±150° with respect to those placed horizontally and vertically at ±90°. The result for the 563 keV $(M2)$ transition is presented in Fig. 2(a) and fitted with a theoretical curve. It includes the calculated A_2, A_4, B_2 and B_4 parameters in accordance with [23] and the experimental oscillation frequency.

The experimental $R(t)$ function for the 563 keV transition, constructed in the same way from all Ge detectors, is shown in Fig. 2(b). It contains similar statistics obtained in about 5 days of measuring time. The experimental data is fitted with the same theoretical curve as the simulation. All parameters are taken in accordance to their theoretical values as deduced using the lowest multipole and assuming no mixing for $A_{2,4}$, and using γ-ray deorientation coefficients for $B_{2,4}$. The resulting experimental frequency, after a full minimization procedure, amounts to $w_0 = 3.26(16)$ MHz. The 316 and 186 keV transitions with $M1$ multipolarity can be summed-up as their A_2B_2 products, taking into account the respective deorientation coefficients, are identical. They result in the $R(t)$ spectrum shown in Fig. 2(c) with $w_0 = 3.28(19)$ MHz. Note that this $R(t)$ function has an opposite phase due to the difference in the multipolarity, resulting in a sign change in A_2. The amplitudes for the 563 keV and the 316 + 186 keV transitions amount to 5.0(6)% and 3.0(6)%, respectively, taking into account the correction for the detector geometry. These are in a good agreement with [23] and the orientation produced in the (d, p) reaction using a polycrystalline host to observe the quadrupole interaction.

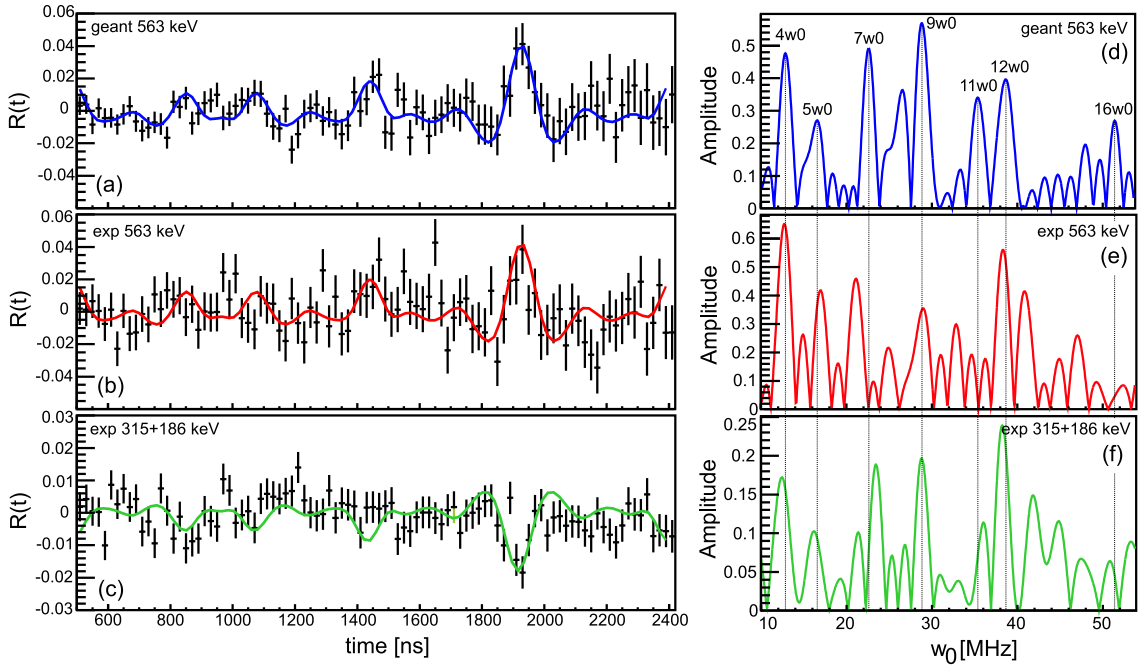

Fig. 2. GEANT simulation (a) compared to the experimental $R(t)$ function (b) for the 563 keV $(M2)$ transition and the sum-up (c) of the 316 and 186 keV $(M1)$ transitions. Fast-Fourier transform on the data is shown for the simulation (d), the $M2$ (e) and sum-up $M1$ (f) γ rays.

A fast-Fourier transform (FFT) was performed on the simulated (Fig. 2(d)) and experimental (Fig. 2(e), (f)) $R(t)$ functions for a time window of about 2 μs. Note that the perturbation factors G_{22}, G_{44}, dependent on the quadrupole interaction and spin, result in different multiples nw_0 of the oscillation frequency w_0 with a different amplitude α_n. The strongest of them for the present case are for $n = 4$, 5, 7, 9, 11, 12, 16, as identified in the FFT on the simulated data (Fig. 2(d)), matching those obtained from the FFT of the experiment. The uncertainty in w_0 from these analyses is taken into account in the final value. It results to $w_0 = 3.27(20)$ MHz, corresponding to a quadrupole coupling constant $\nu_Q = 45.8(28)$ MHz and an oscillation period $T_0 = 1.92(12)$ μs (oscillation quadrupole frequency $\nu_Q^0 = 0.521(32)$ MHz). Taking into account the experimental V_{zz} from ^{63,65}Cu in Cu_2O (see Section 2) and the experimental ν_Q, using Eq. (4), for ^{66m}Cu(6$^-$) a spectroscopic quadrupole moment of $|Q_s| = 18.6(12)$ efm^2 is obtained. Note that using the respective ν_Q from the earlier known ν_Q^0 of ^{63,65}Cu in Cu_2O (see Section 2) and the relation:

$$\left|\frac{Q_s(^{66}\mathrm{Cu}, 6^-)}{Q_s(^{63,65}\mathrm{Cu}, 3/2^-)}\right| = \left|\frac{\nu_Q(^{66}\mathrm{Cu}, 6^-)}{\nu_Q(^{63,65}\mathrm{Cu}, 3/2^-)}\right|, \tag{6}$$

for the $|Q_s(^{66}\mathrm{Cu}, 6^-)|$ a value of 18.67(119) efm^2 is obtained using ^{63}Cu, in a perfect agreement with the value of 18.55(114) efm^2, obtained using ^{65}Cu. The resulting weighted mean of 18.6(12) efm^2, that is the same as obtained using the EFG above, is the final result of our measurement.

4. Discussion

The $9/2^+$ isomers are identified in several isotopic chains (Cr, Fe, Ni, Zn, Ge) of nuclei around ^{68}Ni and their magnetic moment measurements [21] show a predominantly $\nu g_{9/2}$ configuration. The only quadrupole moment measurement on such state was performed on ^{61m}Fe($9/2^+$) ($E_x = 861$ keV, $T_{1/2} = 239(5)$ ns) [22], with a single neutron in the $\nu g_{9/2}$ orbit. The authors reported $|Q_s| = 41(6)$ efm^2 and were uncertain on the sign of the deformation $\beta_2 = -0.21$ or $\beta_2 = +0.24$, as according to mean-field based calculations, using the finite-range Gogny force [22], $I^\pi = 9/2^+$ can be formed from either $K^\pi = 1/2^+$ or $K^\pi = 9/2^+$ band-heads. In a follow-up study of ^{61m}Fe, several high-spin states were reported from the band build on the top of the $9/2^+$ isomer [36] and successfully reproduced in the scope of the particle-triaxial-rotor model with $\beta_2 = +0.24$ ($K^\pi = 1/2^+$ and $Q_0 = +115$ efm^2), thus fixing a prolate shape. On the other hand, the measured quadrupole moment $Q_s(3/2^-)_{\mathrm{g.s.}} = -19.5(4)$ efm^2 for ^{65}Cu [29] corresponds to an oblate shape with $\beta_2 = -0.171(12)$ [37,21]. The experimental magnetic moment of this state [21] indicates that the main contribution in its wave function is from a valence proton in the $\pi p_{3/2}$ orbital, occupying either $\pi[321]1/2$ or $\pi[312]3/2$. Therefore, our Q_s measurement of the ^{66m}Cu(6$^+$) state with a $(\pi p_{3/2} \otimes \nu g_{9/2})$ configuration [23] provides an excellent case to study the interplay between the deformation-driving forces of these two orbitals, knowing $Q_s(\pi p_{3/2})$ and $Q_s(\nu g_{9/2})$.

Mean-field Hartree–Fock–Bogoliubov (HFB) calculations in axial symmetry were performed with the D1N Gogny force [38] and the blocking procedure, as used to describe ^{61m}Fe($9/2^+$) [22]. In the present case, the blocking was applied for protons and neutrons simultaneously. In the case of axial symmetry, the $\pi p_{3/2}$ configuration leads to two possible blocked states for $K_p^\pi = 1/2^-$ and $K_p^\pi = 3/2^-$, while for $\nu g_{9/2}$ five different blocked states with $K_n^\pi = 1/2^+$, $3/2^+$, $5/2^+$, $7/2^+$ and $9/2^+$ are conceivable. Therefore, ten pn blocking configurations are considered: $K^\pi = |K_n^\pi - K_p^\pi|$ being degenerated in energy with $K^\pi = |K_n^\pi + K_p^\pi|$. For each configuration, constrained HFB calculations on the quadrupole deformation were performed, and extended beyond mean-field using the generator coordinate method within the Gaussian-overlap approximation for one degree of freedom [39]. The calculated excitation energies of the ten possible states $(\pi p_{3/2} \otimes \nu g_{9/2})$ as functions of their Q_{20p} are shown in Fig. 3(a), together with the two possible g.s. configurations $(\pi p_{3/2} \otimes \nu p_{1/2})$. As it can be seen, both prolate and oblate shapes can be expected. However, we should stress that all these states result from the coupling of protons and neutrons with the same deformation. This coupling is the lowest in energy. Note that the current approach allows to predict the collective intrinsic-charge quadrupole moment, Q_{20p}, related to Q_s for each K^π through the following equation:

$$Q_s = \frac{3(K^\pi)^2 - I(I+1)}{(I+1)(2I+3)} Q_{20p}. \tag{7}$$

Consequently, the ten energy configurations with double values of K lead to twenty Q_s values. In the following, only eight of them (with the four lowest excitation energies) are considered, namely with $K^\pi = 3^-, 6^-$, $K^\pi = 2^-, 5^-$, $K^\pi = 0^-, 1^-$ and $K^\pi = 1^-, 2^-$. In Fig. 3(b) calculated and experimental Q_s are presented for ^{61m}Fe and ^{65,66m}Cu. Note that, as identified [22,36], for ^{61m}Fe($9/2^+$) only $K^\pi = 1/2^+$ is considered, while for ^{65}Cu, K^π of the $\pi p_{3/2}$ state

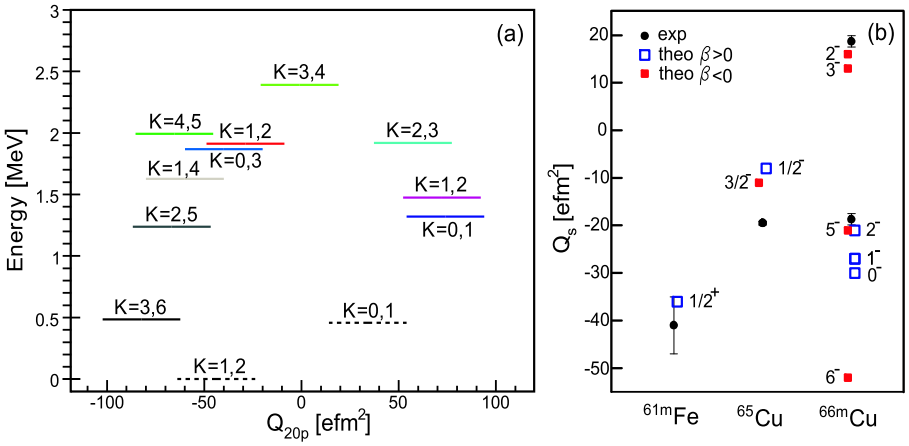

Fig. 3. Excitation energies and Q_{20p} (a) of the predicted isomeric (solid lines) and ground (dashed lines) states in ^{66}Cu. Experimental Q_s (b) for ^{61m}Fe($9/2^-$), ^{65}Cu($3/2^-$) and ^{66m}Cu(6$^-$) (full circles) are compared to the theory for oblate (full squares) and prolate (empty squares) shapes. The theoretical predictions are labelled with their K^π value. Note that the two $K^\pi = 1^-$ configurations have the same Q_s value.

might be $K^\pi = 1/2^-$ or $K^\pi = 3/2^-$. The theoretical predictions for a $K^\pi = 3/2^-$ g.s. result in $Q_s = -11$ efm^2 (with $\beta_2 = -0.11$), while the $K^\pi = 1/2^-$ state is calculated at $E_x = 763$ keV with a $Q_s = -8$ efm^2 ($\beta_2 = +0.08$). Although both reach the experimental Q_s, $I^\pi = 3/2^-$ at minimal (g.s.) energy is constructed on the $K^\pi = 3/2^-$ band-head. The two possible values of the Q_s for the isomeric ^{66m}Cu(6^-) state are plotted in the figure and covered by the expanded theoretical predictions. As can be seen in Fig. 3(a), the first negative parity $K^\pi = 3^-, 6^-$ degenerate states are good isomer candidates. However, the comparison of the experimental and theoretical Q_s values excludes the $K^\pi = 6^-$ state, as shown in Fig. 3(b). Several other possibilities lie in the range of the experimental result with different excitation energies. The $K^\pi = 2^-, 5^-$ pair is predicted higher in energy and should easily decay to the low-lying $K^\pi = 3^-, 6^-$ states. On the prolate side, even if $K^\pi = 0^-, 1^-$ and $K^\pi = 1^-, 2^-$ will be delayed by the difference in deformation, they cannot generate a low-energy $I^\pi = 6^-$ state due to the small K values.

When a proton configuration for odd–even nuclei and a neutron configuration for even–odd ones occur near the same deformation, the corresponding *pn* coupling configuration of the odd–odd neighbours leads to a lower energy state for given orbitals. In the opposite case, one of the isospin configurations imposes to the other ones its shape. Therefore, the *pn* coupling configuration is higher in energy. According to that, the calculations predict ($K^\pi_p = 3/2^- \otimes K^\pi_n = 9/2^+$) to be the most probable isomer candidate, resulting in (oblate $\otimes$ oblate) $K^\pi = 3^-$ state ($\beta_2 = -0.18$), that is in agreement with the experimental spectrum and Q_s value. For this state the negative intinsic Q_{20p} and oblate deformation correspond to a positive Q_s, as can be seen in Fig. 3(b). We can exclude the higher-lying $K^\pi = 2^-, 5^-$ states that are obtained with the improbable $K^\pi_n = 7/2^+$. On the other hand, $K^\pi = 0^-, 1^-$ and $K^\pi = 1^-, 2^-$ (prolate $\otimes$ prolate) contain the coupling of the $K^\pi_p = 1/2^-$ with $K^\pi_n = 1/2^+$ and $3/2^+$, respectively, which are with an opposite deformation.

Note that breaking the time-reversal symmetry to improve the theoretical predictions will lead to energy degeneracy of the pair states with practically unchanged Q_{20p} and respectively Q_s values. Even if the self-consistent calculation leads to two different (energy-deformation) curves, the minima of each energy state will appear at very close Q value compared to the present description [40]. Although the excitation energies might increase by few hundred keV, for example the degeneracy for the $K^\pi = 3^-$ and the $K^\pi = 6^-$ states will be such that $K^\pi = 3^-$ is expected below the $K^\pi = 6^-$ because it minimizes the symmetry breaking. As the ^{65}Cu($3/2^-$) is best reproduced by $K^\pi_p = 3/2^-$ (oblate) and assuming that the 6^- isomer is a $\nu g_{9/2}$ excitation on the ^{65}Cu g.s., the $K^\pi = 3^-$ state, with an oblate shape would be constructed either from $K^\pi_n = 9/2^+$ (oblate) that is most probable in energy or from $K^\pi_n = 1/2^+$ (prolate), that is not energetically favoured. Therefore, this implies that in the newly created *pn* coupled state the protons contribute mainly to oblate shapes. The neutrons, with five different projected K^π_n from prolate to oblate, are responsible for a fast change in this deformation. It is interesting to note, that the neutrons excited to the *sdg* shell couple to the *pf* protons [9,12] due to the same $\nu g_{9/2}$ orbital, that drives to different deformations single-particle states in ^{61m}Fe$_{37}$($9/2^+$) (prolate) and ^{66m}Cu$_{37}$(6^-) (most probably oblate), and is predicted for collective states in ^{66}Fe$_{40}$(2^+) and ^{64}Cr$_{40}$(2^+) [9] to turn the shape into prolate. In our particular case, the proton–neutron coupling with the same (oblate) deformation is favoured. However, one cannot exclude a completely opposite behaviour in the neighbouring neutron rich odd–odd nuclei without more calculations and comparison to the heavier systems where the orbital mixing is much severe.

5. Summary

In this work we have measured for the first time $|Q_s|$ of the 6^- isomeric state in ^{66}Cu. It is the first measurement where an experimental Q_s is obtained using a polycrystalline host with an EFG and is the first Q_s study of a μs isomer in a Cu isotope. This gives not only an experimental methodology to study the whole Cu chain by quadrupole moment measurements of excited states, but also to provide valuable input for the studies in the Ni vicinity. The experimental result reveals an interesting interplay between two different deformation-driving orbitals and suggests that the coupling of deformations of the same type is the most probable scenario. This is in agreement with the mean-field formalism with time reversal symmetry, which have been performed for an odd–odd nucleus. It predicts a positive Q_s sign for an oblate shape, that corresponds to a negative Q_{20p} value. The present formalism applied with time reversal symmetry breaking will provide new results on excitation energy with degeneracy. Moreover, in an adapted QRPA approach for odd–odd systems, the correlations that can be included for the g.s. will allow for a better treatment of the isomeric states. Further experimental work e.g. on the sign and the g.s. Q_s using e.g. polarized beams or on the rotational band build on the top of the isomer as well as on other odd–odd nuclei is essential to increase the theoretical predictive power and elucidate the evolution of deformation.

Acknowledgements

We wish to acknowledge H. Haas for the fruitful discussions on the EFG and the technical staff of the Tandem-ALTO facility of Orsay for their support and assistance. The use of detectors from the Gammapool European Spectroscopy and France–UK (IN2P3/STFC) Loan-Pool Resources through the ORGAM (Orsay Gamma Array) project is gratefully acknowledged. R.L.L. expresses her gratitude to M. Chapellier, M. Izquierdo, K. Chaouchi and J. Cambedouzou for their help in preparing and testing the targets. D.L.B. acknowledges support by the Bulgarian National Science Fund, grants DID-02/16 and DRNF-02/5.

References

[1] O. Sorlin, C. Donzaud, F. Nowacki, J. Angélique, F. Azaiez, C. Bourgeois, V. Chiste, Z. Dlouhy, S. Grévy, D. Guillemaud-Mueller, F. Ibrahim, K.-L. Kratz, M. Lewitowicz, S.M. Lukyanov, J. Mrasek, Y.E. Penionzhkevich, F. de Oliveira Santos, B. Pfeiffer, F. Pougheon, A. Poves, M.G. Saint-Laurent, M. Stanoiu, Eur. Phys. J. A 16 (2003) 55.
[2] S. Raman, C.W. Nestor-JR, P. Tikkanen, At. Data Nucl. Data Tables 78 (2001) 1.
[3] O. Sorlin, S. Leenhardt, C. Donzaud, J. Duprat, F. Azaiez, F. Nowacki, H. Grawe, Z. Dombrádi, F. Amorini, A. Astier, D. Baiborodin, M. Belleguic, C. Borcea, C. Bourgeois, D.M. Cullen, Z. Dlouhy, E. Dragulescu, M. Górska, S. Grévy, D. Guillemaud-Mueller, G. Hagemann, B. Herskind, J. Kiener, R. Lemmon, M. Lewitowicz, S.M. Lukyanov, P. Mayet, F. de Oliveira Santos, D. Pantalica, Y.E. Penionzhkevich, F. Pougheon, A. Poves, N. Redon, M.G. Saint-Laurent, J.A. Scarpaci, G. Sletten, M. Stanoiu, O. Tarasov, C. Theisen, Phys. Rev. Lett. 88 (2002) 092501.
[4] C. Guénaut, G. Audi, D. Beck, K. Blaum, G. Bollen, P. Delahaye, F. Herfurth, A. Kellerbauer, H.-J. Kluge, J. Libert, D. Lunney, S. Schwarz, L. Schweikhard, C. Yazidjian, Phys. Rev. C 75 (2007) 044303.
[5] M. Hannawald, T. Kautzsch, A. Wöhr, W.B. Walters, K.L. Kratz, V.N. Fedoseyev, V.I. Mishin, W. Böhmer, B. Pfeiffer, V. Sebastian, Y. Jading, J.L.U. Köster, H.L. Ravn, ISOLDE Collaboration, Phys. Rev. Lett. 82 (1999) 1391.
[6] A.N. Deacon, M. Hannawald, T. Kautzsch, A. Woehr, W.B. Walters, K.-L. Kratz, V.N. Fedoseyev, V.I. Mishin, W. Boehmer, B. Pfeiffer, V. Sebastian, Y. Jading, U. Köster, J. Lettry, H.L. Ravn, ISOLDE Collaboration, Phys. Lett. B 622 (2005) 151.
[7] S.J. Freeman, R.V.F. Janssensa, B.A. Brown, M.P. Carpenter, S.M. Fischer, N.J. Hammond, M. Honma, T. Lauritsen, C.J. Lister, T.L. Khoo, G. Mukherjee, D. Seweryniak, J.F. Smith, B.J. Varley, M. Whitehead, S. Zhu, Phys. Rev. C 69 (2004) 064301.
[8] A.N. Deacon, S.J. Freeman, R.V.F. Janssens, M. Honma, M.P. Carpenter, P. Chowdhury, T. Lauritsen, C.J. Lister, D. Seweryniak, J.F. Smith, S.L. Tabor, B.J. Varley, F.R. Xu, Phys. Rev. C 76 (2007) 054303.

[9] E. Caurier, F. Nowacki, A. Poves, Eur. Phys. J. A 15 (2002) 145.
[10] D. Hirata, K. Sumiyoshi, I. Tanihata, Y. Sugahara, T. Tachibana, H. Toki, Nucl. Phys. A 616 (1997) 438c.
[11] Y. Aboussir, J.M. Pearson, A.K. Dutta, F. Tondeur, At. Data Nucl. Data Tables 61 (1995) 127.
[12] S. Lunardi, S.M. Lenzi, F.D. Vedova, E. Farnea, A. Gadea, N. Marginean, D. Bazzacco, S. Beghini, P.G. Bizzeti, A.M. Bizzeti-Sona, D. Bucurescu, L. Corradi, A.N. Deacon, G. de Angelis, E. Fioretto, S.J. Freeman, M. Ionescu-Bujor, A. Iordachescu, P. Mason, D. Mengoni, G. Montagnoli, D.R. Napoli, F. Nowacki, R. Orlandi, G. Pollarolo, F. Recchia, F. Scarlassara, J.F. Smith, A.M. Stefanini, S. Szilner, C.A. Ur, J.J. Valiente-Dobon, B.J. Varley, Phys. Rev. C 76 (2007) 034303.
[13] M. Block, C. Bachelet, G. Bollen, M. Facina, C.M. Folden, A.A.K.C. Guénaut, D.J. Morrissey, G.K. Pang, A. Prinke, R. Ringle, J. Savory, P. Schury, S. Schwarz, Phys. Rev. Lett. 100 (2008) 132501.
[14] D. Pauwels, O. Ivanov, N. Bree, J. Büscher, T.E. Cocolios, J. Gentens, M. Huyse, A. Korgul, Y. Kudryavtsev, R. Raabe, M. Sawicka, I. Stefanescu, J.V. de Walle, P.V. den Bergh, P.V. Duppen, W.B. Walters, Phys. Rev. C 78 (2009) 041307(R).
[15] I. Stefanescu, G. Georgiev, F. Ames, J. Äystö, D.L. Balabanski, G. Bollen, P.A. Butler, J. Cederkäl, N. Champault, T. Davinson, A.D. Maesschalck, P. Delahaye, J. Eberth, D. Fedorov, V.N. Fedosseev, L.M. Fraile, S. Franchoo, K. Gladnishki, D. Habs, K. Heyde, M. Huyse, O. Ivanov, J. Iwanicki, J. Jolie, B. Jonson, T. Kröll, R. Krücken, O. Kester, U. Köster, A. Lagoyannis, L. Liljeby, G.L. Bianco, B.A. Marsh, O. Niedermaier, T. Nilsson, M. Oinonen, G. Pascovici, P. Reiter, A. Saltarelli, H. Scheit, D. Schwalm, T. Sieber, N. Smirnova, J.V.D. Walle, P.V. Duppen, S. Zemlyanoi, N. Warr, D. Weisshaar, F. Wenander, Phys. Rev. Lett. 98 (2007) 122701.
[16] I. Stefanescu, G. Georgiev, D.L. Balabanski, N. Blasi, A. Blazhev, N. Bree, J. Cederkäll, T.E. Cocolios, T. Davinson, J. Diriken, J. Eberth, A. Ekström, D. Fedorov, V.N. Fedosseev, L.M. Fraile, S. Franchoo, K. Gladnishki, M. Huyse, O. Ivanov, V. Ivanov, J. Iwanicki, J. Jolie, T. Konstantinopoulos, T. Kröll, R. Krücken, U. Köster, A. Lagoyannis, G.L. Bianco, P. Maierbeck, B.A. Marsh, P. Napiorkowski, N. Patronis, D. Pauwels, G. Rainovski, P. Reiter, K. Riisager, M. Seliverstov, G. Sletten, J.V. de Walle, P.V. Duppen, D. Voulot, N. Warr, F. Wenander, K. Wrzosek, Phys. Rev. Lett. 100 (2008) 112502.
[17] M. Honma, T. Otsuka, T. Mizusaki, M. Hjorth-Jensen, Phys. Rev. C 80 (2009) 064323.
[18] T. Otsuka, T. Suzuki, R. Fujimoto, H. Grawe, Y. Akaishi, Phys. Rev. Lett. 85 (2005) 232502.
[19] G. Georgiev, I. Matea, D.L. Balabanski, J.M. Daugas, F.O. Santos, S. Franchoo, F. Ibrahim, F.L. Blanc, M. Lewitowicz, G.L. Bianco, S. Lukyanov, V. Meot, P. Morel, G. Neyens, Y.E. Penionzhkevich, A. Saltarelli, O. Sorlin, M. Stanoiu, M. Tarisien, N. Vermeulen, D. Verney, D. Yordanov, Eur. Phys. J. A 30 (2006) 351.
[20] G. Georgiev, G. Neyens, M. Hass, D.L. Balabanski, C. Bingham, C. Borcea, N. Coulier, R. Coussement, J.M. Daugas, G.D. France, F. de Oliveira Santos, M. Górska, H. Grawe, R. Grzywacz, M. Lewitowicz, H. Mach, I. Matea, R.D. Page, M. Pfützner, Y.E. Penionzhkevich, Z. Podolyák, P.H. Regan, K. Rykaczewski, M. Sawicka, N.A. Smirnova, Y.G. Sobolev, M. Stanoiu, S. Teughels, K. Vyvey, J. Phys. G: Nucl. Part. Phys. 28 (2002) 2993.
[21] N.J. Stone, At. Data Nucl. Data Tables 90 (2005) 75.
[22] N. Vermeulen, S.K. Chamoli, J.M. Daugas, M. Hass, D.L. Balabanski, J.P. Delaroche, F. de Oliveira-Santos, G. Georgiev, M. Girod, G. Goldring, H. Goutte, S. Grévy, I. Matea, P. Morel, B.S.N. Singh, Y.E. Penionzhkevich, L. Perrot, O. Perru, S. Péru, O. Roig, F. Sarazin, G.S. Simpson, Y. Sobolev, I. Stefan, C. Stodel, D.T. Yordanov, G. Neyens, Phys. Rev. C 75 (2007) 051302(R).
[23] J. Bleck, R. Butt, K.H. Lindenberger, W. Ribbe, W. Zeitz, Nucl. Phys. A 197 (1972) 620.
[24] E.Y. Tonkov, Compounds and Alloys under High Pressure, Gordon and Breach Science Publishers, Amsterdam, 1998.
[25] K. Alder, R.M. Steffen, Annu. Rev. Nucl. Sci. 14 (1964) 403.
[26] E. Dafni, R. Bienstock, M.H. Rafailovich, G.D. Sprouse, At. Data Nucl. Data Tables 23 (1979) 315.
[27] R.M. Steffen, K. Alder, The Electromagnetic Interaction in Nuclear Spectroscopy, North-Holland, Amsterdam, 1975.
[28] H.W. de Wijn, J.L. de Wildt, Phys. Rev. 150 (1966) 200.
[29] R.M. Sternheimer, Phys. Rev. 164 (1967) 10.
[30] B. Effenberger, W. Kunold, W. Oesterle, M. Schneider, L.M. Simons, R. Abela, J. Wüest, Z. Phys. A 309 (1982) 77.
[31] C.P. Massolo, M. Rentería, J. Desimoni, A.G. Biliboni, Phys. Rev. B 37 (1988) 4743.
[32] T. Lippmann, J.R. Schneider, Acta Crystallogr. A 56 (2000) 575.
[33] E. Davni, M. Hass, H.H. Bertschat, C. Broude, F. Davidovsky, G. Goldring, P.M.S. Lesser, Phys. Rev. Lett. 50 (1983) 1652.
[34] E. Dafni, J. Bendahan, C. Broude, G. Goldring, M. Hass, E. Naim, M.H. Rafailovich, C. Chasman, O.C. Kistner, S. Vajda, Phys. Rev. Lett. 53 (1984) 2473.
[35] www.info.cern.ch/asd/geant/, 2010.
[36] N. Hoteling, W.B. Walters, R.V.F. Janssens, R. Broda, M.P. Carpenter, B. Fornal, A.A. Hecht, M. Hjorth-Jensen, W. Królas, T. Lauritsen, T. Pawat, D. Seweryniak, J.R. Stone, X. Wang, A. Wöhr, J. Wrzesinski, S. Zhu, Phys. Rev. C 77 (2008) 044314.
[37] http://cdfe.sinp.msu.ru, 2010.
[38] F. Chappert, M. Girod, S. Hilaire, Phys. Lett. B 668 (2008) 420.
[39] J.P. Blaizot, J.F. Berger, J. Decharge, M. Girod, Nucl. Phys. A 591 (1995) 435.
[40] S. Péru, et al., 2010, in preparation.